ISSN 2411-3336; e-ISSN 2541-9404

JOURNAL OF MINING INSTITUTE

Zapiski Gornogo instituta

Journal homepage: pmi.spmi.ru

*Research article*

# Origin of carbonate-silicate rocks of the Porya Guba (the Lapland-Kolvitsa Granulite Belt) revealed by stable isotope analysis ($\delta^{18}O$, $\delta^{13}C$)

**Dmitrii P. KRYLOV** ✉, **Ekaterina V. KLIMOVA**

*Institute of Precambrian Geology and Geochronology RAS, Saint Petersburg, Russia*

***How to cite this article***: Krylov D.P., Klimova E.V. Origin of carbonate-silicate rocks of the Porya Guba (the Lapland-Kolvitsa Granulite Belt) revealed by stable isotope analysis ($\delta^{18}O$, $\delta^{13}C$). Journal of Mining Institute. 2024. Vol. 265, p. 3-15. EDN GISHQG

***Abstract.*** Carbonate-silicate rocks of unclear origin have been observed in granulites of the Porya Guba of the Lapland-Kolvitsa Belt within the Fennoscandinavian Shield. The present work aims to reconstruct possible protoliths and conditions of metamorphic transformation of these rocks based on oxygen and carbon isotopic ratios combined with phase equilibria modeling. Isotope analysis and lithochemical reconstructions suggest that carbonate-silicate rocks of the Porya Guba represent metamorphosed sediments (possibly marls) with the isotopic composition corresponding to the Precambrian diagenetically transformed carbonates ($\delta^{18}O \approx 17.9$ ‰, SMOW and $\delta^{13}C \approx -3.4$ ‰, PDB). The chemical composition varies depending on the balance among the carbonate, clay, and clastic components. Significant changes of the isotopic composition during metamorphism are caused by decomposition reactions of primary carbonates (dolomite, siderite, and ankerite) producing $CO_2$ followed by degassing. These reactions are accompanied by $\delta^{18}O$ and $\delta^{13}C$ decrease of calcite in isotopic equilibrium with $CO_2$ down to 15 ‰ (SMOW) and –6 ‰ (PDB), respectively. The isotopic composition is buffered by local reactions within individual rock varieties, thus excluding any pronounced influence of magmatic and/or metasomatic processes.

***Keywords***: carbonate-silicate rocks; stable isotopes; metamorphism; inorganic carbon cycle; isotope fractionation; Rayleigh distillation

***Acknowledgment***. The work was financed by Russian Science Foundation, grant N 22-27-00275, https://rscf.ru/en/project/22-27-00275/.

***Received: 07.02.2023*** ***Accepted: 20.06.2023*** ***Online: 06.09.2023*** ***Published: 29.02.2024***

**Introduction.** The carbonate-silicate geochemical cycle (the inorganic carbon cycle [1]) includes the processes of weathering, sedimentation (with silicate to carbonate transformations), metamorphism and volcanic activity (with conversion of carbonates to silicates). Over an interval of several million years or more, this cycle controls the balance of $CO_2$ during interactions of the atmosphere, hydrosphere, crust, and mantle of the Earth and largely determines global climate changes [2-4]. Carbonate-silicate rocks in metamorphic complexes (hereafter, for brevity, the obsolete term calciphyres is used) represent a sequence of phase transformations in the cycle stages associated with formation of the carbonate substrate, metamorphism, degassing, and the release of significant amounts of $CO_2$ into the atmosphere [5-7]. Phase reactions in the carbonate-silicate cycle are accompanied by isotopic reactions, and the ratios of stable isotopes ($^{18}O/^{16}O$,$^{13}C/^{12}C$), as well as "unconventional" isotopes of magnesium, calcium silicon and titanium can serve as the most important geochemical tracers [8-10] and provide an opportunity to estimate the influence of different reservoirs on the composition of gases, temperatures of processes, as well as $CO_2/H_2O$ balance in the atmosphere, hydrosphere and gases of deep origins. Nevertheless, stable isotope data have been mostly limited to sedimentary carbonate rocks of low metamorphic degrees; the sources

of matter and conditions of calciphyre transformations within highly metamorphosed (granulite) terranes have been less studied [11, 12].

Ancient granulite terranes which are widely developed within the shields and in the crystalline basement of platforms provide important evidence on the composition and degree of transformation of the continental crust formed during early stages of the Earth history [13-15]. The Lapland-Kolvitsa Granulite Belt is a part of the Fennoscandinavian Shield, which in recent years provides a scientific testing ground for various geological models and concepts [16-18]. The Paleoproterozoic events that led to the formation of rock associations of the Lapland-Kolvitsa Belt have also been widely manifested in the adjacent tectonic structures, for example in the rocks of the Belomorian Mobile Belt [19-21].

Within the Lapland-Kolvitsa Granulite Belt among other formations, rare outcrops of calciphyres have been observed, so far with unclear origin. A general description, sporadic measurements of the chemical composition [22-24] and carbon isotope ratios [25] suggest a sedimentary precursor and possible biogenic component of some rocks of the belt, but the alternation of calciphyres with presumably metaintrusive rocks makes their assignment to metasediments doubtful. The aim of the present work is to study oxygen and carbon isotopic compositions accomplished by the phase equilibria modeling of the Porya Guba calciphyres, and to reconstruct possible protolith origins and metamorphic conditions. The results of the isotopic measurements are supplemented by new data on chemical and phase compositions of the rocks.

**Methods.** *The isotope composition measurements*. Standard procedures [26, 27] were used to extract $CO_2$ from carbonates (100 % $H_3PO_4$) and $O_2$ from silicates (the fluorination followed by the conversion to $CO_2$). The extraction yield (at least 98 %) was controlled by measuring the gas volume, the completeness of the conversion was checked by measuring the residual oxygen pressure. $CO_2$ isotope ratios were determined on the SIRA-9 mass spectrometer (VG-Isogas). The entire extraction and measurement cycle for each sample was repeated at least twice. In addition, the oxygen isotopic composition of the in-lab $CO_2$ standard was determined every 4-5 experiments. Calcite samples calibrated relative to the NBS-18 standard were used to control the carbonate determinations. The accepted acid fractionation factor of calcite ($T$ = 25 °C) is 1.01049 [28]. Samples of quartz and potassium feldspar calibrated relative to NBS-28 were used to control the results of the silicate measurements. Isotopic data are given according to the conventional δ-notation relative to V-SMOW (for oxygen) and PDB (for carbon) standards: $\delta = [R_{sam}/R_{std} - 1]1000$, where $R_{sam}/R_{std}$ is the ratio of heavy and light isotopes in the sample and the standard. The average error of the values $\delta^{18}O$ is 0.07 ‰, $\delta^{13}C$ 0.05 ‰ (1σ). Sample preparation and measurement of oxygen isotope composition were performed at the Institute of Petrology and Mineralogy (Bonn).

The fractionation of isotopes between phases $A$ and $B$ is quantified by the value $\alpha_{AB} = R_A/R_B = (\delta_A + 1000)/(\delta_B + 1000)$. The value $\alpha_{AB}$ can be obtained using so-called "β-factors", so that provided isotopic equilibrium $10^3 \ln\alpha_{AB}(T) = 1000\ln\beta_A(T) - 1000\ln\beta_B(T)$. Temperatures of the isotopic equilibrium are determined by the measured isotopic ratios of phases given the temperature dependences of the β-factors. For the purposes of the present work, $\beta(T)$ dependences in the form of the cubic polynomials determined on the basis of isotopic frequency shifts [29] have been adopted.

*Calculation of phase equilibria*. Phase equilibria were modeled for the system $SiO_2$-$TiO_2$-$Al_2O_3$-FeO-MgO-CaO-$Na_2O$-$K_2O$-$H_2O$-$CO_2$ (STAFMCNK-$H_2O$-$CO_2$) using the Perple_X (version 6.9, http://www.perplex.ethz.ch/) [30, 31] and GeoPS [32] software. For the fluid ($H_2O$-$CO_2$), the equation of state and thermodynamic database ([33], modified in 2004) have been adopted. The calculations account for the phases present in the rocks, their possible precursors and transformation products. The results of X-ray fluorescence spectrometry (Philips PW-1480 device) with an analytical error less than 3 % were taken as the input data to calculate the phase equilibria (pseudosections).

*Journal of Mining Institute.* 2024. Vol. 265. P. 3-15


Compositions of individual phases were determined on the JEOL JXA-8230 device (IGGD RAS) at 15 kV accelerating voltage, 20 nA electron probe current, and 10 μm beam diameter. Calcite $CO_2$ content was quantified after drying the sample (for 1 h at $T = 105$ °C) using value of the gas extracted during reaction with 10 % hydrochloric acid solution. Termination of the carbonate decomposition was recorded by the cessation of the gas release.

**Geological background and rock composition.** The metacarbonate rocks had been distinguished as part of the lower sequence of the Kolvitsa granulite zone (Ploskotundrovskaya series [22]), and are also noted at the southeastern end of the Lapland block (Salny and Tuadash tundras). The rocks are mostly observed in the Porya Guba area of the Kandalaksha Bay of the White Sea on the Medvezhy Island and the western coast of the Porya Guba, where outcrops of calciphyres are traced for 10-15 km along the strike (NW-SE). This paper presents data on the rocks from the Medvezhy Island and the Tamarkina Luda Island (West of the Porya Guba, Fig.1). Within the outcrop on the Medvezhy Island, calciphyres form interlayers (extending up to several tens of meters) with a thickness from few centimeters to 50-60 cm, alternating with mafic schists (two-pyroxene, garnet-two-pyroxene, amphibole-diopside, actinolite, scapolite-bearing, etc.), acidic granulites, and variably migmatized gneisses. In places, the schists and gneisses contain sulfide mineralization. The rocks of the interbedded calciphyres and mafic schists are characterized by boudinage and delamination structures due to the different resistance of carbonates and silicates.

Metamorphic age of the rocks from the granulite complex are estimated from 1925 Ma (the beginning of metamorphism) to 1870 Ma (its termination) [34]. The protolith formation refers to the Early Proterozoic, although there is evidence of the pre-Proterozoic (the Late Archean?) age [35].

The calciphyres are presented by medium to large-grained, gray, banded rocks, usually of granoblastic (heterogranoblastic) texture. According to the mineral composition, two main groups can be distinguished within the calciphyre layers:

• Calciphyres, dominated by calcite, monoclinic pyroxene (diopside), garnet (up to 13 vol.%), quartz (0.1-0.5 mm, 5-15 %), sometimes plagioclase (0.01-1.5 mm). Calcite occurs as large polysynthetic grains up to 2-3 mm. Large colorless segregations of diopside (0.3-2 mm, reaching 30 % of the rock volume) have been replaced by tremolite and phlogopite. Garnet poikiloblasts (up to 1 cm) are dominated by the grossular-andradite series, with a small content of pyrope and almandine. However, in rocks with the significant plagioclase content (reaching 10-15 vol.%) garnet (sometimes relic, up to 5-7 vol.%) is dominated by almandine with pyrope. Magnesite, dolomite, sometimes olivine (forsterite), titanite or ilmenite, and apatite are present as accessories (< 5 %). For the sake of brevity, this variety will be referred to as the diopside calciphyres (*di*-calciphyres).

• Calciphyres dominated by forsterite, calcite with a small amount of monoclinic pyroxene. Within some rocks idioblastic (up to a few mm) calcite segregations are found. Olivine grains (0.3-0.5 mm) are replaced by serpentine (0.2-0.3 mm). Other secondary hydroxyl-bearing minerals are also present: mainly mica, chlorite, epidote, and amphibole (actinolite-tremolite, up to 0.5 mm). It should be noted that, despite the significant MgO content in the olivine-bearing varieties of the studied calciphyres, dolomite is usually found as relics. Apatite, titanite, ilmenite, and spinel (hercinite) are observed as accessories. This variety of the carbonate-silicate rocks is further referred to as the olivine calciphyres (*ol*-calciphyres).

In addition to the mineral composition, the two calciphyre varieties differ also by the content of the major oxides (Table 1). The olivine calciphyres have significantly higher MgO/(MgO + CaO) ratio (about 0.4) if compared with the calciphyres of the first group (less than 0.1). FeO and MnO contents of the *ol*-calciphyres are slightly lower than in the *di*-calciphyres, higher alkaline contents are noted in the olivine-bearing varieties. Differences in the concentrations of other components (including $CO_2$, $SiO_2$, $Al_2O_3$) are insignificant.

**Journal of Mining Institute.** 2024. Vol. 265. P. 3-15
EDN GISHQG


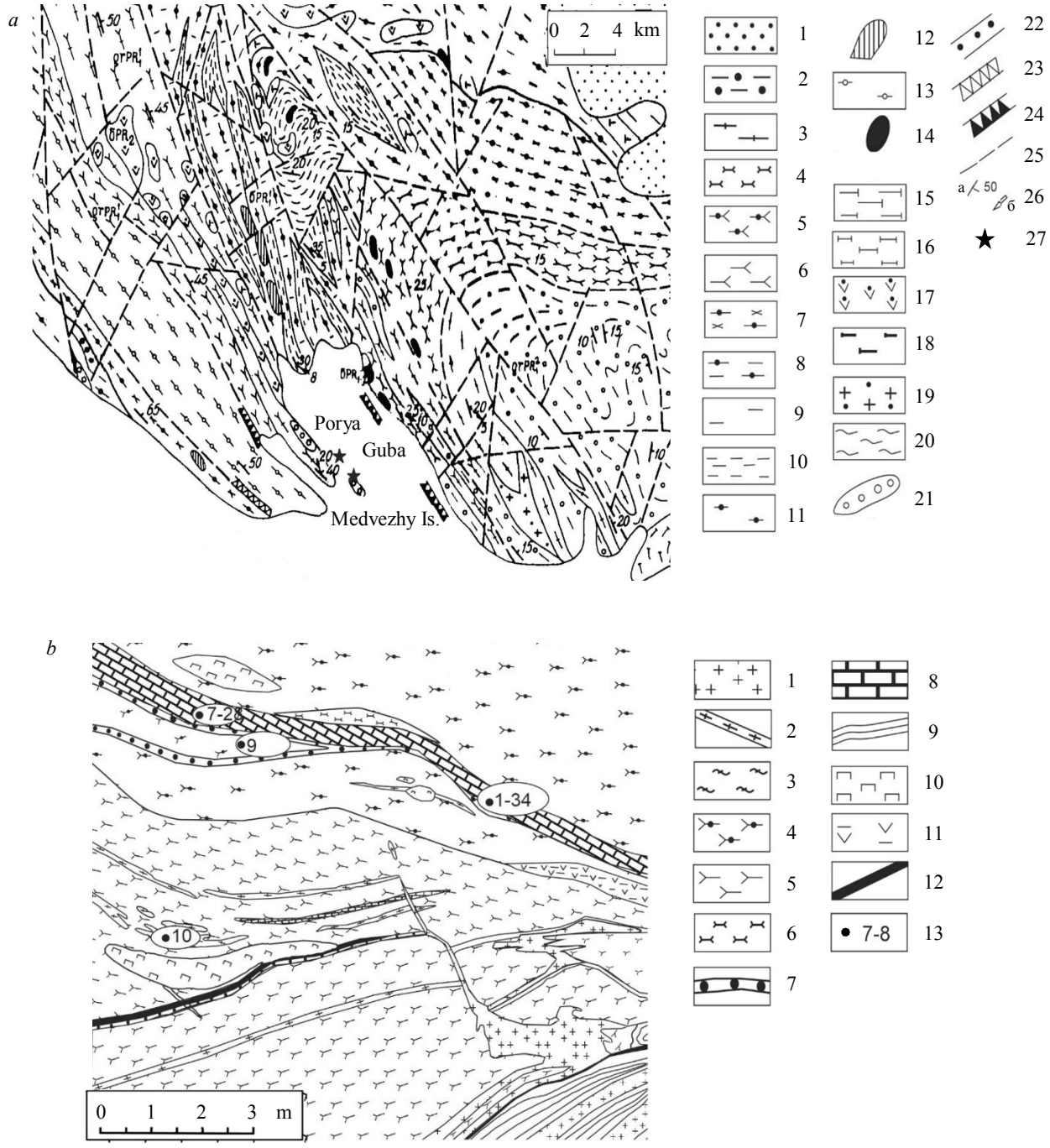


Fig.1. Geological map of the Porya Guba area (*a*) and sketch of the detailed area on the Medvezhy Island (*b*) modified after [22]:

*a* – Porya Guba: 1 – Quaternary sediments; 2-7 – supracrustal formations: 2 – sillimanite-granite-biotite gneisses, 3 – acidic granulites, 4 – plagioclase-orthopyroxene crystalline schists, 5 – two-pyroxene mafic schists, 6 – plagioclase-granite-pyroxene mafic schists, 7 – garnet-amphibolites; 8, 9 – gneiss complex of the granulite framing: 8 – biotite-amphibole gneisses, 9 – gneisses (unclassified); 10, 11 – diaphtorites over granulites: 10 – garnet-bearing gneisses with relict pyroxenes, 11 – garnet-pyroxene amphibolites; 12-19 – magmatic rocks: 12 – druzites (13 – plagioclasites, metagabbro-anorthosites, 14 – norites and pyroxenites, 15 – enderbites, 16 – charnockites, 17 – hornblende peridotites, 18 – unclassified ultrabasites, 19 – alkaline gneissic-granites); 20-24 – other rocks: 20 – migmatites, 21 – calciphyres, 22 – conglomerates, 23 – eruptive breccia, 24 – tectonic breccia with sulfide cement; 25 – tectonic discontinuaties; 26 – structural attitudes (a – schistocity, b – linearity); 27 – sampling sites (the Medvezhy Island and the Tamarkina Luda Island);

*b* – the Medvezhy Island locality: 1 – pegmatites; 2 – acidic granulites; 3 – charnockite-migmatites; 4 – amphibole-diopside plagioclase mafic schists with garnet; 5 – garnet-two-pyroxene plagioclase mafic schists; 6 – plagioclase-hyperstene mafic schists; 7 – quartzites; 8 – calciphyres; 9 – biotite gneisses with sillimanite; 10 – clinopyroxenites; 11 – actinolite schists; 12 – gabbro-diabases; 13 – sampling spots (Table 1)

*Journal of Mining Institute.* 2024. Vol. 265. P. 3-15


*Table 1*

**The whole-rock composition of the calciphyres and spatially related Porya Guba mafic schists**

| Rock | *di*-calciphyres | | | *ol*-calciphyres | | | Mafic schists | | |
|---|---|---|---|---|---|---|---|---|---|
| | Sample number | | | | | | | | |
| | 7 | 28 | 13 | 8 | 1 | 3 | 12 | 9 | 10 |
| $SiO_2$ | 29.97 | 20.36 | 19.97 | 33.07 | 19.15 | 22.05 | 31.36 | 57.53 | 52.61 |
| $TiO_2$ | 0.27 | 0.07 | 0.17 | 0.13 | 0.20 | 0.61 | 0.47 | 0.76 | 0.67 |
| $Al_2O_3$ | 4.04 | 2.69 | 0.10 | 2.55 | 1.45 | 1.55 | 2.20 | 13.41 | 9.66 |
| FeO | 5.77 | 4.40 | 3.77 | 2.91 | 2.56 | 2.89 | 1.71 | 7.66 | 10.56 |
| MnO | 0.39 | 0.23 | 0.38 | 0.18 | 0.33 | 0.63 | 0.76 | 0.09 | 0.15 |
| MgO | 2.55 | 1.87 | 1.69 | 18.52 | 19.52 | 17.61 | 16.62 | 6.87 | 11.32 |
| CaO | 36.87 | 42.33 | 43.25 | 25.38 | 28.87 | 29.11 | 25.55 | 5.94 | 10.12 |
| $Na_2O$ | 0.25 | 0.15 | 0.27 | 0.31 | 0.67 | 1.11 | 1.29 | 3.94 | 2.29 |
| $K_2O$ | 0.10 | 0.62 | 0.05 | 0.10 | 0.59 | 0.99 | 0.57 | 1.62 | 0.93 |
| $P_2O_5$ | 0.18 | 0.09 | 0.20 | 0.05 | 0.04 | 0.05 | 0.33 | 0.05 | 0.07 |
| $CO_2$ | 19.60 | 25.77 | 28.00 | 16.79 | 20.63 | 20.02 | 17.54 | – | – |
| LOI | – | 0.29 | – | 0.97 | 4.70 | 3.82 | 0.44 | 2.12 | 1.59 |
| Total | 99.99 | 98.87 | 97.85 | 100.96 | 98.71 | 100.44 | 98.84 | 99.99 | 99.97 |
| MgO/(MgO + CaO) | 0.06 | 0.04 | 0.04 | 0.42 | 0.40 | 0.38 | 0.39 | 0.54 | 0.53 |

*Notes*: sample 13 – the Tamarkina Luda Island, others – the Medvezhy Island; LOI – loss on ignition (105 °C).

**Oxygen and carbon isotopes.** Measured isotopic ratios of calcite ($\delta^{18}O$ and $\delta^{13}C$ relative to SMOW and PDB, respectively) and silicates ($\delta^{18}O$) are given in Table 2. The $\delta^{18}O$ value of calcite in the calciphyres vary from 15.0 до 17.8 ‰ (the mean value at 16.44±0.92 ‰) with $\delta^{13}C$ varying from –3.6 to –6.2 ‰ (the mean at –4.90±0.89 ‰), suggesting the sedimentary nature of the rocks. At the same time, average $\delta^{18}O$ of calcite from the diopside calciphyres is 17.05 (±0.61) ‰, whereas average $\delta^{18}O$ of calcite in the olivine-bearing varieties is lower, 15.68 (±0.59) ‰. Average $\delta^{13}C$ values of calcite are –4.35 (±0.65) and –5.58 (±0.67) ‰, respectively. Calcite $\delta^{18}O$ and $\delta^{13}C$ increase following the increase of the calcite content in the rock (which is expressed for example, as a linear dependence of $\delta^{18}O_{cal} \approx 0.15CO_2 + 13.02$ wt.%, $R^2 = 0.7$). In the limit of the pure calcite rock ($CO_2 = 44$ wt.%), $\delta^{18}O_{cal}$, according to this relationship, is estimated at 19.6 ‰, which corresponds to the isotopic composition of the Precambrian diaphtorised carbonate sediments [36, 37]. Another noted pattern – the relationship $\delta^{18}O$ and $\delta^{13}C$ of calcite – may reflect metamorphic degassing of the rocks. Representative isotopic analyses of the calciphyres taken from the Tamarkina Luda Island for comparison follow the same pattern.

Temperature dependences of the stable isotope fractionations are determined based on the β-factors (the reduced partition function ratios):

$$\ln\beta = \frac{1}{N_q}\sum_{\{q\}}\left[\frac{1}{N}\sum_{i=1}^{3N_{at}}\ln\left(\frac{\nu^*_{q,i}}{\nu_{q,i}}\frac{\sinh(h\nu_{q,i}/2kT)}{\sinh(h\nu^*_{q,i}/2kT)}\right)\right],$$

where $\nu_{q,i}$ are the vibrational frequencies with the wave vector $q$ and phonon branch index $i$ from 1 to $3N_{at}$; $N_{at}$ is the number of atoms in a unit cell; $T$ temperature, K; $h$ and $k$ – the Planck and Boltzmann constants; $N$ is the number of atoms undergoing isotopic substitution; $N_q$ is the number of vectors $q$ considered in the summation; the superscript * refers to the heavier isotope.

The β-factors (calcite, quartz, monoclinic pyroxene, olivine, and garnet) between 0 and 1500 °C are interpolated by the cubic polynomials against $x = 10^6/T^2 : 1000\ln\beta^{18}O = ax + bx^2 + cx^3$ [29]. The vibration frequencies of the isotopologues of the studied phases were determined by the frozen phonon method (CRYSTAL software: https://www.crystal.unito.it/) within the density functional theory (DFT).

*Table 2*

**Isotopic composition of pure fraction separates**

| Sample number | Measured isotopic composition ($\delta O^{18}_{SMOW}$, $\delta C^{13}_{PDB}$) | | | | | | *T*, °C | | | | *F* | $CO_2(i)$ |
|---|---|---|---|---|---|---|---|---|---|---|---|---|
| | $\delta^{18}O_{cal}$ | $\delta^{13}C_{cal}$ | $\delta^{18}O_{qtz}$ | $\delta^{18}O_{cpx}$ | $\delta^{18}O_{ol}$ | $\delta^{18}O_{oth}$ | *qtz-cal* | *ol-cal* | *cpx-cal* | Others | | |
| *di*-calciphyres | | | | | | | | | | | | |
| 7 | 16.50 | –4.62 | 17.14 | 13.10 | – | $14.47_{grt}$ | 990 | – | 620 | $856_{grt\text{-}qtz}$ | 0.70 | 27.96 |
| 28 | 17.54 | –4.20 | 18.07 | – | – | – | 1110 | – | – | – | 0.90 | 28.54 |
| 13 | 17.78 | –3.57 | 19.85 | 16.45 | – | $16.32_{grt}$ | 430 | – | 810 | $701_{grt\text{-}qtz}$ | 0.96 | 29.25 |
| 21 | 16.41 | –5.31 | 17.85 | – | – | – | 570 | – | – | – | 0.69 | 39.69 |
| 34 | 17.03 | –4.05 | 17.65 | – | – | – | 1010 | – | – | – | 0.80 | 38.24 |
| *ol*-calciphyres | | | | | | | | | | | | |
| 8 | 15.02 | –6.06 | – | – | 12.04 | – | – | 520 | – | – | 0.49 | 34.35 |
| 1 | 16.31 | –5.32 | – | – | 12.51 | – | – | 410 | – | – | 0.67 | 30.82 |
| 3 | 16.03 | –4.76 | – | – | 14.75 | – | – | 990 | – | – | 0.63 | 32.02 |
| Mafic schists | | | | | | | | | | | | |
| 12 | 15.37 | –6.18 | – | – | 12.07 | – | – | 470 | – | – | 0.53 | 32.95 |
| 9 | – | – | – | 12.11 | – | $13.42_{pl}$ | – | – | – | $670_{pl\text{-}cpx}$ | – | – |
| 10 | – | – | – | 11.60 | – | $13.38_{pl}$ | – | – | – | $480_{pl\text{-}cpx}$ | – | – |
| Coefficients of temperature dependence of the β-factors | | | | | | | | | | | | |
| | $\beta^{18}O_{cal}$ | – | $\beta^{18}O_{qtz}$ | $\beta^{18}O_{cpx}$ | $\beta^{18}O_{ol}$ | $\beta^{18}O_{pl}$ | – | – | – | – | – | $\beta^{18}O_{CO_2}$ |
| *a* | 11.6603 | – | 12.6764 | 10.0399 | 9.50807 | 11.478 | – | – | – | – | – | 15.1896 |
| *b* | –0.3544 | – | –0.3543 | –0.205 | –0.1654 | –0.457 | – | – | – | – | – | –0.7068 |
| *c* | 0.00908 | – | 0.00841 | 0.00401 | 0.0018 | 0.0077 | – | – | – | – | – | 0.0206 |

*Notes*: *F* – fraction of $CO_2$, remaining in calcite after degassing; $CO_2(i)$ – $CO_2$ content in a rock prior to degassing (see Table 1). For samples 21, 34 the measured $CO_2$ concentrations are 27.22 and 30.50, respectively.

The value of $\delta^{18}O$ within the silicate fraction of the calciphyres (quartz, pyroxene, olivine, garnet, Table 2) depends both on the isotopic composition of the carbonate fraction (the higher $\delta^{18}O_{cal}$, generally the higher $\delta^{18}O$ of each particular phase), and the $^{18}O/^{16}O$ fractionation between different phases depending on temperature. $\delta^{18}O$ variation of quartz in the *di*-calciphyres is 17.1-19.9 ‰, pyroxene 13.1-16.5 ‰. $\delta^{18}O$ values of olivine from the *ol*-calciphyres vary between 12.0 and 14.8 ‰. Generally, the decrease of $\delta^{18}O$ values occurs in the sequence quartz-calcite-(garnet-pyroxene). The lack of equilibrium between minerals is indicated by the large scatter of temperatures calculated from the distribution of isotopes between different phases of each particular sample (Table 2). For example, temperatures calculated using the quartz-calcite isotope geothermometer vary from 430 °C (sample 13) to 990 °C (sample 7) and 1110 °C (sample 34), calcite-clinopyroxene from 620 to 810 °C (on two samples).

Within rocks without carbonates, both at contacts with calciphyres and at some distance (5-10 m) the evolved $\delta^{18}O$ (reaching 11.6-13.5 ‰ for pyroxene and plagioclase) is also observed.

**Revealing primary composition of metamorphic rocks.** The oxygen and carbon isotopic ratios imply primary sedimentary nature of the Porya Guba calciphyres and possibly, of the entire rock sequence studied (NW coast of the Porya Guba). Hence, the phase compositions of primary sediments were reconstructed based on the rock chemistry. Using the Perple_X program (see the methods), the restored ("model") phase composition of rocks in the conditions of the sedimentation (25 °C, 1 bar) was calculated (Table 3).

Sediments chemically corresponding to the *di*-calciphyres contained 70-85 wt.% of the carbonate fraction dominated by calcite (reaching 78 %), with subordinate amounts of dolomite (up to 10 %) and ankerite (up to 15 %). The clastic component includes quartz (reaching 22 wt.%), while kaolin dominates in the clay fraction (up to 9 wt.%). The detrital component (rutile and titanite) content is estimated at 0.1-0.2 %. The primary composition of sediments transformed into the *ol*-calciphyres (mostly forsterite) was characterized by significant amount of dolomite within carbonate fraction (up to 62 wt.%) together with ankerite (up to 8 %), siderite (up to 4 %), and magnesite (less than 1 %). Calcite content did not exceed 35 wt.%.

*Journal of Mining Institute.* 2024. Vol. 265. P. 3-15


*Table 3*

**Reconstructed composition of rocks in the conditions of sedimentation, wt.%**

| Rock | Sample number | | | | | | | | |
|---|---|---|---|---|---|---|---|---|---|
| | *di*-calciphyres | | | *ol*-calciphyres | | | | Mafic schists | |
| | 7 | 28 | 13 | 8 | 1 | 3 | 12 | 9 | 10 |
| Carbonate component | | | | | | | | | |
| Calcite | 44.3 | 74.4 | 78.0 | – | 35.1 | 32.4 | 20.4 | – | 5.3 |
| Dolomite | 10.0 | – | – | 61.7 | 24.9 | 20.5 | 33.1 | 15.4 | 2.0 |
| Siderite | – | – | – | 3.5 | – | – | – | 9.7 | – |
| Magnesite | – | – | – | 0.4 | – | – | – | 4.3 | – |
| Ankerite | 14.9 | – | 5.5 | – | 7.2 | 7.9 | 4.6 | – | 3.3 |
| Carbonate total | 69.3 | 74.4 | 83.5 | 65.6 | 67.2 | 60.8 | 58.1 | 29.4 | 10.6 |
| Clastic component | | | | | | | | | |
| Quartz | 21.7 | 0.3 | 14.6 | 22.2 | – | – | 9.2 | 43.3 | 5.8 |
| Rutile | 0.2 | – | 0.2 | 0.1 | – | 0.6 | 0.4 | 0.6 | – |
| Clinopyroxene | – | 4.8 | – | – | – | – | – | – | – |
| Titanite | – | 0.2 | – | – | – | – | – | – | 1.5 |
| Zeolites | – | 18.3 | – | – | – | – | – | – | – |
| Ilmenite | – | – | – | – | 0.4 | – | – | – | – |
| Clastic total | 21.9 | 23.6 | 14.9 | 22.3 | 0.4 | 0.6 | 9.6 | 43.9 | 7.3 |
| Clay fraction, amphibole, mica, other phyllosilicates | | | | | | | | | |
| Kaolinite | 8.8 | – | 0.8 | 4.8 | – | – | – | 26.7 | – |
| Talc | – | – | – | – | – | 1.9 | 5.3 | – | – |
| Glaucophane | – | – | – | – | – | 3.3 | 10.8 | – | 26.7 |
| Chlorite | – | 2.0 | 0.8 | – | – | – | – | – | 2.9 |
| Mica | – | – | – | 7.4 | – | 2.1 | – | – | 7.3 |
| Serpentine | – | – | – | – | 20.3 | 10.3 | – | – | – |
| Stylpnomelan | – | – | – | – | 12.1 | 21.0 | 16.2 | – | – |
| Chloritoid | – | – | – | – | – | – | – | – | 10.2 |
| Actinolite | – | – | – | – | – | – | – | – | 35.0 |
| Total fraction | 8.8 | 2.0 | 1.6 | 12.1 | 32.4 | 38.6 | 32.3 | 26.7 | 82.1 |

*Notes*. Composition calculated from data in Table 1 at ambient conditions $T = 298.15$ °C, $P = 1$ bar (Werami module of the Perple_X software [30]). $CO_2$ content calculated from the measured composition accounting the degree of degassing $F$ and given at Table 2; in the absence of the respective data, calculations were performed under conditions of the volatile saturation ($H_2O > 5$ %).

Sedimentary rocks currently represented by mafic schists, contained less than 30 wt.% carbonates (as reconstructed with $CO_2$ excess), and probably were dominated either by the clastic components (up to 43 % quartz, sample 9) or the clay components (sample 10). Oxygen isotopic variations of the sediments in interaction with seawater at 25 °C are estimated at 31.8±2.3 ‰ (probable oxygen isotopic composition prior to the sediments lithification).

**Metamorphic phase equilibria of the calciphyres.** Phase equilibrium diagrams with the stability fields of phase associations in *P-T* coordinates (pseudosections) were constructed accounting for chemical composition of representative samples of the diopside calciphyres from the Medvezhy and the Tamarkina Luda islands, the olivine calciphyres, and garnet-pyroxene plagioclase schists (see Table 1). The pseudosections constrain *P-T* conditions of phase transformations and in particular, probable temperatures of fluid component releases, which is essential when evaluating isotopic composition of rocks. Close spatial relations of the studied rocks imply similar *P-T* conditions of metamorphism, which should correspond to the intersection of the stability fields observed in different mineral associations of the samples. For clarity, the results of pseudosection modeling are presented without considering components presented in insignificant amounts (Fig.2).

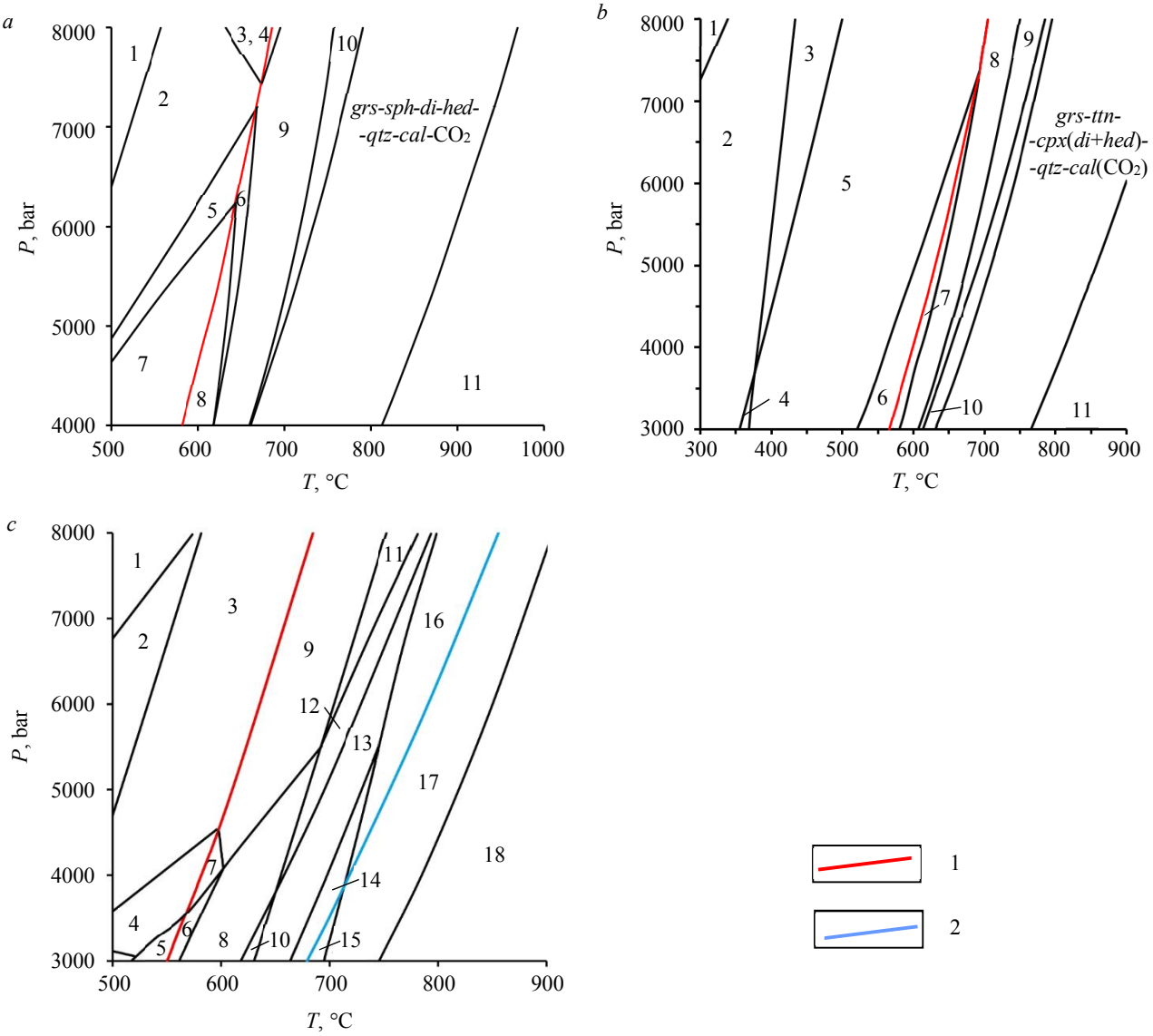


Fig.2. Phase *P-T*-diagrams (pseudosections) constructed from the analysis of the representative Porya Guba calciphyres:

*a:* sample 7. Anhydrous projection. Stable phases: 1 – *alm-grs-ttn-di-qtz-cal-dol*; 2 – *alm-ttn-di-qtz-hc-cal-dol*; 3 – *alm-ttn-di-qtz-spr-cal-dol*; 4 – *alm-ttn-di-qtz-spr-cal*-$CO_2$; 5 – *alm-di-qtz-ilm-hc-cal-dol*; 6 – *alm-di-qtz-ilm-hc-cal*-$CO_2$; 7 – *alm-crd-di-qtz-ilm-cal-dol*; 8 – *alm-crd-di-qtz-ilm-cal*-$CO_2$; 9 – *alm-ttn-di-qtz-hc-cal*-$CO_2$; 10 – *alm-grs-ttn-di-qtz-cal*-$CO_2$; 11 – *grs-ttn-di-hed-wo-cal*-$CO_2$;

*b*: sample 13. Anhydrous projection. Stable phases: 1 – *grs-ttn-di-hed-qtz-arg-ank*; 2 – *grs-ttn-di-hed-qtz-cal-ank*; 3 – *alm-ttn-di-hed-qtz-cal-ank*; 4 – *grs-ilm-di-hed-qtz-cal-ank*; 5 – *alm-ilm-di-hed-qtz-cal-ank*; 6 – *alm-ilm-di-fa-qtz-cal-ank*; 7 – *alm-ilm-di-fa-qtz-cal*-$CO_2$; 8 – *alm-ilm-di-hed-qtz-cal*-$CO_2$; 9 – *alm-ttn-di-hed-qtz-cal*-$CO_2$; 10 – *sil-ttn-di-hed-qtz-cal*-$CO_2$; 11 – *grs-ttn-di-hed-wo-cal*-$CO_2$;

*c*: sample 8. Projection including $H_2O$. Stable phases: 1 – *alm-ky-di-tr-qtz-ilm-mgs-dol*; 2 – *alm-an-di-tr-qtz-ilm-mgs-dol*; 3 – *alm-en-di-tr-an-qtz-ilm-dol*; 4 – *alm-en-di-act-an-qtz-ilm-dol*; 5 – *fa-en-di-an-qtz-ilm-dol-act*; 6 – *fa-en-di-an-ilm-dol*-$CO_2$-*act*; 7 – *alm-en-di-an-ilm-dol*-$CO_2$-*act*; 8 – *fa-en-di-tr-an-ilm-dol*-$CO_2$; 9 – *alm-en-di-tr-an-ilm-dol*-$CO_2$; 10 – *fo-fa-di-tr-an-ilm-dol*-$CO_2$; 11 – *alm-en-di-tr-ilm-hc-dol*-$CO_2$; 12 – *fa-en-di-tr-ilm-hc-dol*-$CO_2$; 13 – *fo-fa-di-tr-ilm-hc-dol*-$CO_2$; 14 – *fo-fa-di-clin-ilm-hc-dol*-$CO_2$; 15 – *fo-fa-di-clin-ilm-hc-cal*-$CO_2$; 16 – *fo-fa-di-ilm-hc-dol*-$H_2O$-$CO_2$; 17 (observed association) – *fo-fa-di-ilm-hc-cal*-$H_2O$-$CO_2$; 18 – *fo-fa-di-hc-usp-cal*-$H_2O$-$CO_2$

Phase abbreviations. Carbonates: *ank* – ankerite; *cal* – calcite; *dol* – dolomite; *mgs* – magnesite; *sid* – siderite; *arg* – aragonite. Silicates: *qtz* – quartz; *ol* – olivine (*fo* – forsterite, *fa* – fayalite); *cpx* – monoclinic pyroxene (*di* – diopside, *hed* – hedenbergite); *opx* – rhombic pyroxene (*en* – enstatite, *hyp* – hypersten); *grt* – garnet (*alm* – almandine, *grs* – grossular); *pl* – plagioclase (*an* – anorthite); *spr* – sapphirin; *crd* – cordierite; *sil* – sillimanite; *ky* – kyanite; *wo* – wollastonite; *amp* – amphibole (*act* – actinolite, *gl* – glaucophane, *hrn* – hornblende, *tr* – tremolite); mica (*bt* – biotite, *mu* – muscovite, *phl* – phlogopite); oxides: *spl* – spinel (*hc* – hercinite, *usp* – ulvospinel); *rt* – rutile; *ttn* – titanite; *ilm* – ilmenite

1 – lines of monovariant equilibria limiting the appearance of $CO_2$; 2 – lines limiting calcite appearance

**Journal of Mining Institute.** 2024. Vol. 265. P. 3-15


Decarbonatization reactions that accompany phase transformations of all the calciphyres studied deserve special attention to explain the change in the isotopic composition of rocks, because these reactions cause isotopic fractionation of both oxygen and carbon; the isotopic fractionation factors between $CO_2$ and solid phases are significant even at elevated temperatures; large volume increase associated with the formation of fluid components causes complete or partial removal of $CO_2$.

Considering the *di*-calciphyres, $CO_2$ release is caused by the decomposition reactions of dolomite or ankerite, which becomes unstable as temperature increases:

$$CaMg(CO_3)_2(dol) + SiO_2 = CaCO_3(cal) + MgSiO_3(cpx) + CO_2; \quad (1)$$

$$CaMg(CO_3)_2(dol) + 2SiO_2 = > CaMgSiO_3(cpx) + 2CO_2. \quad (2)$$

If carbonates with iron (ankerite, sample 13) prevail in the source rock at low temperatures, carbon dioxide is released for example, by the reaction

$$CaFe(CO_3)_2\ (sid) + SiO_2 = CaCO_3(cal) + FeSiO_3(cpx) + CO_2. \quad (3)$$

The source of silica can be quartz as well as other silicates including:

$$CaMg(CO_3)_2(dol) + Fe_3Al_2(SiO_4)_3(alm) =$$
$$= CaCO_3(cal) + 2FeSiO_3(cpx) + MgSiO_3(cpx) + FeAl_2O_4(spl) + CO_2; \quad (4)$$

$$3CaMg(CO_3)_2(dol) + CaMg(SiO_3)_2(di) = 4CaCO_3(cal) + 2Mg_2SiO_4(fo) + 2CO_2. \quad (5)$$

In the *di*-calciphyres of the Medvezhy Island (sample 7) at pressures below 6 kbar, the decarbonatization reactions start within the range of 580-630 °C (Fig.2, *a*, red lines ). The simplified anhydrous projection of the system is shown for clarity. At higher pressures, the onset temperature of $CO_2$ release also rises (e.g., if $P = 8$ kbar, the onset of $CO_2$ release shifts to $T \approx 700$ °C). By the sequence of phase reactions, primary sediments (see Table 1) transform into the observed *grs-ttn-di-hed-qtz-cal* association which at 8 kbar is stable from 790 to 970 °C (at another pressure the stability field shifts by about 30 °C/kbar). At lower temperatures, hedenbergite is stable rather than almandine and at higher temperatures, wollastonite appears instead of quartz.

Association of the *di*-calciphyres from the Tamarkina Luda Island (sample 13) is *cal-cpx*(*di* + *hed*)-*-grt*(*grs*)-*qtz-ttn*. The onset of decarbonatization at a reduced pressure is possible from 560 °C ($P = 3$ kbar). At higher pressures, the temperature of $CO_2$ release increases to 705 °C ($P = 8$ kbar), with an estimated $\partial T/\partial P$ gradient of approximately 29 °C/kbar (Fig.2, *b*). Similar to the Medvezhy Island diopside calciphyres (sample 7), the stability field of the observed *grs-ttn-cpx-qtz-cal* association with increasing temperature is limited by the association with wollastonite instead of quartz. It is noteworthy that for these rocks, carbonates which are stable up to temperatures of approximately 570-650 °C consist of calcite and ankerite rather than dolomite (as in sample 7) and accordingly, decarbonatization is caused by the decomposition of ankerite by a reaction similar to (3).

The *ol*-calciphyres (sample 8, Fig.2, *c*). The observed *fo-fa-di-ilm-hc-cal* association remains in equilibrium with the fluid components ($H_2O + CO_2$) starting from 690 °C at 3 kbar or 860 °C at 8 kbar; the upper stability boundary is 750 to 905 °C, respectively. The lower-temperature association includes dolomite, relics of which are observed in thin sections; in the higher-temperature association *fo-fa-di-usp-hc-cal*-($H_2O$-$CO_2$) ulvospinel is formed at the expense of ilmenite. It should be noted that, in contrast to diopside calciphyres, the beginning of decarbonatization (marked by red line in Fig.2, *c*) does not lead to the total breakdown of dolomite, and calcite becomes stable only from 680 °C (3 kbar) to 860 °C (8 kbar), which coincides with the lower temperature limit at which the observed association remains stable (Fig.2, *c*, blue line).

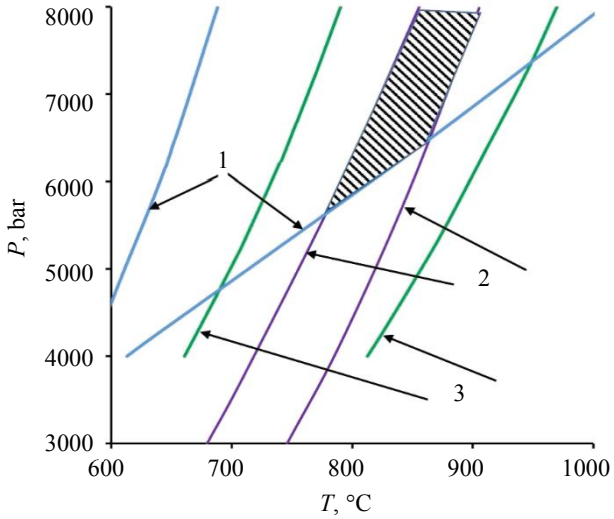


Fig.3. Stability fields of mineral associations of the calciphyres and mafic schists. The intersection area of all observed associations is shaded

1 – *grt-px*-schists; 2 – *ol*-calciphyres; 3 – *di*-calciphyres

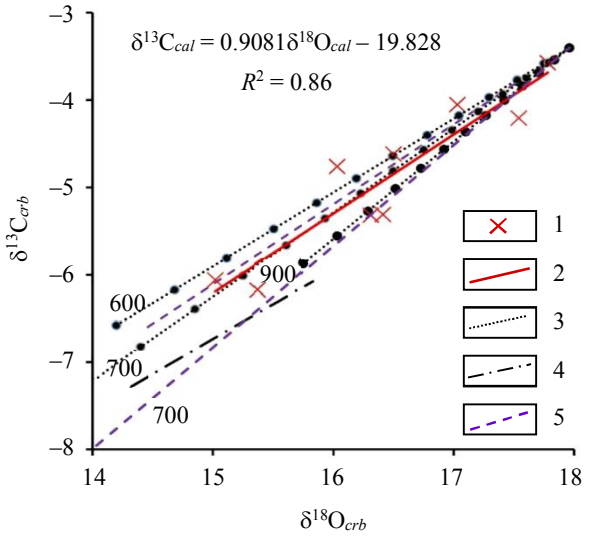


Fig.4. Isotopic ratios $^{18}O/^{16}O$ and $^{13}C/^{12}C$ of calcite from the Porya Guba calciphyres

1 – data points; 2 – linear array, plotted according to the results of isotopic analysis; 3 – calculated according to equation (6) for isotopic fractionations (the values of the oxygen fractionation factor $\alpha^{18/16}$ *cal*-$CO_2$ given $T$ = 600, 700 and 900 °C are estimated at 1.00411, 1.00311 and 1.00242, respectively; $\alpha^{18/16}$ *dol*-$CO_2$ – 1.00303, 1.0025, 1.0018, respectively [29]; the carbon fractionation factor $\alpha^{13/12}$ *cal*-$CO_2$ at the given $T$ are 1.0035, 1.0033, 1.0027; $\alpha^{13/12}$ *dol*-$CO_2$ – 1.00306, 1.0029, 1.00246 [29]); 4 – calculated provided isotopic equilibrium of $CO_2$ with carbonates and silicates at 600 °C; 5 – calculated provided isotopic equilibrium of $CO_2$ with dolomite at $T$ = 500, 700 °C

All the observed mineral associations are stable within *PT*-conditions determined by the intersection of the equilibrium fields for different rocks (Fig.3). At the minimum possible pressures (5.5-6 kbar), the temperature limiting the stability of all associations is 740-870 °C. If the metamorphic pressure is higher, temperature estimates increase ($dT/dP \approx$ 30-40 °C/kbar), and at $P$ = 8 kbar the temperature interval at which all the observed associations can coexist is 860-910 °C.

**Discussion.** *Evolution of the isotope composition during metamorphism.* A significant correlation between $\delta^{13}C$ and $\delta^{18}O$ values of calcite ($R^2$ = 0.86; Fig.3) is generally observed (within samples composing all varieties of the studied calciphyres). The reactions of $CO_2$ release characterizing metamorphic transformations of the calciphyre precursors are accompanied by fractionation of oxygen and carbon isotopes with the restite (solid phase residue after gas extraction) depletion in the heavy isotope (1000lnα between $CO_2$ and carbonates and (or) silicates is always greater than zero for the equilibrium oxygen isotope fractionation, and for temperature above ca. 150-200 °C for the carbon isotope fractionation also [29]). Provided constant volume, continuous removal of the released $CO_2$ from the system is likely, so that the change in the isotopic composition of the solid phases can be evaluated with equation of the Rayleigh's distillation, the latter expressed by the relation [38] for isotope fractionation:

$$\delta_r^f - \delta_r^i = 1000(F^{(\alpha-1)} - 1), \qquad (6)$$

where $F$ stands for the mole fraction of an element remaining in the restite after gas extraction; δ expresses the isotopic ratio of an element (oxygen, carbon) in a solid; α is the isotopic fractionation factor between fluid and solid phases: $(^{18}O/^{16}O)$fluid/$(^{18}O/^{16}O)$restite; $f$ and $i$ denote values after gas release and before gas release, respectively.

The linear array expressing simultaneous changes of oxygen and carbon isotopic ratios agrees with the analytical dependence of $\delta^{13}C_{cal}$ and $\delta^{18}O_{cal}$ (Fig.4), provided that the isotopic equilibrium of $CO_2$ and the produced carbonate (calcite and (or) dolomite) was maintained during degassing, isotopic reactions of $CO_2$ with carbonates were hardly accompanied by isotopic reactions with silicates. The latter assumption can be justified by the disagreement of the calculated array considering isotopic equilibrium involving silicates with the analytical data (dashed line in Fig.4).

**Journal of Mining Institute.** 2024. Vol. 265. P. 3-15


In addition, the measured distribution of oxygen isotopes between calcite and silicates (see Table 2) significantly deviates from the equilibrium distribution. In the absence of the isotope equilibrium with silicates, values of $F$ for oxygen and carbon coincide ($F_C = F_O$ [39]). The *cal*-$CO_2$ isotope fractionation in the latter case corresponds to 700 °C, which is wholly endorsed by the estimates of decarbonatization temperatures obtained from phase relations modeling (with the construction of $P$-$T$ pseudosections).

The averaged dependence combines analytical data over all samples, including the diopside and olivine calciphyres. Some deviations of the analytical points can be caused by fluctuation of the fractionation values (variations of the decarbonatization temperature, changes of the composition of carbonates in equilibrium with $CO_2$ of the olivine calciphyres). In particular, however, the measured variations of $\delta^{18}O$ and $\delta^{13}C$ reflect the degree of distillation $F$ of equation (6) provided the same isotopic composition of carbonate at the initial stage of distillation ($F$ = 1, the beginning of $CO_2$ release) and similar degassing temperature (at $T$ = 700 °C the values of $\delta^{18}O_{cal}$ = 17.96 and $\delta^{13}C_{cal}$ = –3.4 ‰ closely follow the analytical data).

Depleted $\delta^{18}O$ values of calcite from the *ol*-calciphyres relative to $\delta^{18}O$ of calcite from the *di*-calciphyres with a general trend $\delta^{18}O$ vs $\delta^{13}C$ can be interpreted as a result of larger degassing degree of the former. Thus, maximum values of $\delta^{18}O_{cal}$ = 17.78 and $\delta^{13}C_{cal}$ = –3.57 ‰ (sample 13) reflect initial stages of the distillation ($F$ = 0.96), whereas minimum values of $\delta^{18}O_{cal}$ = 15.02 and $\delta^{13}C_{cal}$ = –6.06 ‰ (sample 8) correspond to more advanced distillation ($F$ = 0.5). The results are consistent with the process of decarbonatization with decomposition of dolomite (or Fe-carbonate, sample 13) producing calcite (see Fig.2, *b*) due to a series of sequential reactions with removal of the released $CO_2$. Temperature of the degassing obtained from the isotopic analysis is supported by the phase modeling ($T$ = 700 °C at $P \approx$ 8 kbar).

Close agreement of the analytical data in the $\delta^{13}C$ vs $\delta^{18}O$ diagram with the Rayleigh distillation model suggests that the isotopic composition of the removed $CO_2$ and the remaining carbonate was controlled by the equilibrium exchange between the remaining carbonate (calcite) after carbon dioxide extraction and the continuously removed gas. The process occurred without isotopic exchange with silicates. Isotopic composition of the produced $CO_2$ in equilibrium with calcite vary depending on the degree of degassing, from $\delta^{18}O$ = 21.9 and $\delta^{13}C$ = –1.0 ‰ ($F \approx$ 1) up to 18.9 and –3.7 ‰ ($F \approx$ 0.5), respectively. The integrated (batch) isotopic composition of the resulting $CO_2$ falls between these values and is determined by the material balance relations. In case of insignificant change of the fractionation during decarbonatization, the isotopic composition of all formed $CO_2$ is estimated at $\delta^{18}O$ =19.9 and $\delta^{13}C$ = –2.2 ‰ ($F$ = 0.5).

Equilibrium of the released gas with calcite without silicates [40] does not restrict $F$ by the so-called calc-silicate limit ($F$ = 0.6 [38]), and the minimum values of the measured isotope ratios correspond to degassing degree at about 0.5 (the *ol*-calciphyres).

**Conclusion.** The results of oxygen and carbon isotope analysis indicate that the Porya Guba calciphyres and the intercalated mafic schists with the evolved $\delta^{18}O$ and $\delta^{13}C$ resulted from metamorphism of sedimentary rocks (limestones, marls, and graywackes). Lithochemical reconstructions suggest marly sediments as the precursors for the carbonate-silicate rocks, while chemical composition of the former varied depending on the ratio of clay, carbonate, and clastic components. Carbonates comprise 58-84 wt.% (in the sediment precursors of the calciphyres) and 10-30 wt.% (in the possible protoliths of the mafic schists). The isotopic composition of the sediments ($\delta^{18}O$ 17.9 ‰ SMOW and $\delta^{13}C$ –3.4 ‰ PDB) lies within the values typical for the Precambrian diagenetically transformed sedimentary carbonates [36, 37, 41] without any influence of both organic carbon [25] and carbon of the magmatic origin [42].

The most significant shifts in the isotopic composition during metamorphism of the rocks are due to the sequence of reactions producing $CO_2$ following decomposition of dolomite or other carbonates (siderite, ankerite), which become unstable when temperature rises to 700 °C

($P \approx 8$ kbar) and are replaced by magnesium/iron silicates (e.g., monoclinic pyroxene, garnet). The degassing was accompanied by the simultaneous reduction of the calcite $\delta^{18}O$ and $\delta^{13}C$ as a result of the isotopic fractionation (accompanied by the Rayleigh distillation) yielding values of 15.0 and –6.2 ‰, respectively (half of the initial $CO_2$ removed) and producing the linear relationship $\delta^{18}O$ vs $\delta^{13}C$. The isotopic composition of the carbon dioxide released (and possibly added to the atmosphere) is estimated at 20 ‰ (SMOW) and –2 ‰ (PDB).

The shift of the calcite isotopic composition thus reflects different degrees of degassing, which in turn, depends on the composition of the parent rocks. For example, the more dolomite prior to metamorphism contained in a sedimentary rock, the higher the degree of degassing. In the olivine calciphyres (MgO up to 20 wt.%), $\delta^{18}O$ and $\delta^{13}C$ are generally lower than in the diopside calciphyres. At the same time, variations in the isotopic composition of calcite of the interbedded rocks are consistent with the internal (local) control of the emitting fluid [40] and contradict the large-scale interaction with any external (deep or surface) reservoir. Among other things, our results are not consistent with the possibility of mixing (assimilation) of the studied carbonate rocks with magmatic rocks and/or metasomatic transformations during the skarn formation.

It can be noted that at metamorphic temperatures below 650-700 °C dolomite remains stable and the observed dolomite calciphyres of the Kolvitsa granulite zone [24], chemically similar to the olivine calciphyres considered in the present work, might be the “precursors” of olivine calciphyres at lower peak metamorphic temperatures.

## REFERENCES

1. Berner R.A., Lasaga A.C., Garrels R.M. The carbonate-silicate geochemical cycle and its effect on atmospheric carbon dioxide over the past 100 million years. *American Journal of Science*. 1983. Vol. 283. Iss. 7, p. 641-683. DOI: 10.2475/ajs.283.7.641

2. Groppo C., Rolfo F., Castelli D., Connolly J.A.D. Metamorphic $CO_2$ production from calc-silicate rocks via garnet-forming reactions in the CFAS-$H_2O$-$CO_2$ system. *Contributions to Mineralogy and Petrology*. 2013. Vol. 166, p. 1655-1675. DOI: 10.1007/s00410-013-0947-5

3. Catling D.C., Kasting J.F. Atmospheric Evolution on Inhabited and Lifeless Worlds. Cambridge: Cambridge University Press, 2017, p. 579. DOI: 10.1017/9781139020558

4. Sorokhtin N.O., Nikiforov S.L., Kozlov N.Ye. Crust-mantle branch of the global carbon cycle and origin of deep-seated hydrocarbons. *Vestnik of MSTU*. 2018. Vol. 21. N 1, p. 61-79 (in Russian). DOI: 10.21443/1560-9278-2018-21-1-61-79

5. Brovarone A.V., Tumiati S., Piccoli F. et al. Fluid-mediated selective dissolution of subducting carbonaceous material: Implications for carbon recycling and fluid fluxes at forearc depths. *Chemical Geology*. 2020. Vol. 549. N 119682. DOI: 10.1016/j.chemgeo.2020.119682

6. Deep Carbon: Past to present / Ed. by Orcutt B.N., Daniel I., Dasgupta R. Cambridge: Cambridge University Press, 2020, p. 669. DOI: 10.1017/9781108677950

7. Stagno V. Carbon, carbides, carbonates and carbonatitic melts in the Earth’s interior. *Journal of the Geological Society*. 2019. Vol. 176. Iss. 2, p. 375-387. DOI: 10.1144/jgs2018-095

8. Skublov S.G., Rumyantseva N.A., Qiuli Li et al. Zircon xenocrysts from the Shaka Ridge record ancient continental crust: New U-Pb geochronological and oxygen isotopic data. *Journal of Earth Science*. 2022. Vol. 33. N 1, p. 5-16. DOI: 10.1007/s12583-021-1422-2

9. Levashova E.V., Skublov S.G., Oitseva. T.A. et al. First Age and Geochemical Data on Zircon from Riebeckite Granites of the Verkhnee Espe Rare Earth-Rare Metal Deposit, East Kazakhstan. *Geochemistry International*. 2022. Vol. 60. N 1, p. 3-18. DOI: 10.31857/S0016752522010083

10. Rumyantseva N.A., Skublov S.G., Vanshtein B.G. et al. Zircon from Gabbroids of the Shaka Ridge (South Atlantic): U-Pb Age, Oxygen Isotope Ratios and Trace Element Composition. *Proceedings of the Russian Mineralogical Society*. 2022. S. CLI. N 1, p. 44-73 (in Russian). DOI: 10.31857/S0869605522010099

11. Satish-Kumar M., Miyamoto T., Hermann J. et al. Pre-metamorphic carbon, oxygen and strontium isotope signature of high-grade marbles from the Lützow-Holm Complex, East Antarctica: apparent age constraints of carbonate deposition. *Geological Society, London, Special Publications*. 2008. Vol. 308. Iss. 1, p. 147-164. DOI: 10.1144/SP308.7

12. Thaworndumrongsakul P., Booth J., Nantasin P., Kim Y. Metamorphic Evolution of Calc-silicate Body Enclosed in Charnockitic Gneiss at West Ongul Island, Lützow-Holm Complex, East Antarctica. *IOP Conference Series: Earth and Environmental Science*. 2021. Vol. 837. N 012015. DOI: 10.1088/1755-1315/837/1/012015

13. Jacobs J., Mikhalsky E., Henjes-Kunst F. et al. Neoproterozoic geodynamic evolution of easternmost Kalahari: Constraints from U-Pb-Hf-O zircon, Sm-Nd isotope and geochemical data from the Schirmacher Oasis, East Antarctica. *Precambrian Research*. 2020. Vol. 342. N 105553. DOI: 10.1016/j.precamres.2019.105553

14. Gusev N.I., Sergeeva L.Yu., Larionov A.N., Skublov S.G. Relics of the eoarchean continental crust of the Anabar shield, Siberian craton. *Petrology*. 2020. Vol. 28. N 2, p. 115-138. DOI: 10.31857/S086959032002003X

15. Gusev N.I., Sergeeva L.Yu., Skublov S.G. Evidence of subduction of the paleoproterozoic oceanic crust in the Khapchan belt of the Anabar shield, Siberian craton. *Petrology.* 2021. Vol. 29. N 2, p. 115-135. DOI: 10.31857/S0869590321020047

16. Il'chenko V.L., Afanasieva E.N., Kaulina T.V. et al. Litsa Uranium ore occurrence (Arctic zone of the Fennoscandian Shield): new results of petrophysical and geochemical studies. *Journal of Mining Institute.* 2022. Vol. 255, p. 393-404. DOI: 10.31897/PMI.2022.44

17. Kudryashov N.M., Udoratina O.V., Kalinin A.A. et al. U-Pb (SHRIMP-RG) age of zircon from rare-metal (Li, Cs) pegmatites of the Okhmylk deposit of the Kolmozero-Voron'ya greenstone belt (northeast of the Fennoscandian shield). *Journal of Mining Institute.* 2022. Vol. 255, p. 448-454. DOI: 10.31897/PMI.2022.41

18. Smolkin V.F., Mokrushin A.V., Bayanova T.B. et al. Magma feeding paleochannel in the Monchegorsk ore region: geochemistry, isotope U-Pb and Sm-Ndanalysis (Kola region, Russia). *Journal of Mining Institute.* 2022. Vol. 255, p. 405-418. DOI: 10.31897/PMI.2022.48

19. Salimgaraeva L.I., Skublov S.G., Berezin A.V., Galankina O.L. Fahlbands of the Keret archipelago, White Sea: the composition of rocks and minerals, ore mineralization. *Journal of Mining Institute.* 2020. Vol. 245, p. 513-521. DOI: 10.31897/ PMI.2020.5.2

20. Melnik A.E., Skublov S.G., Rubatto D. et al. Garnet and zircon geochronology of the Paleoproterozoic Kuru-Vaara eclogites, northern Belomorian Province, Fennoscandian Shield. *Precambrian Research*. 2021. Vol. 353. N 106014. DOI: 10.1016/j.precamres.2020.106014

21. Skublov S.G., Berezin A.V., Salimgaraeva L.I. Eclogites of the Belomorian mobile belt: geological-petrological and isotope-geochemical age criteria. *Geochemistry International.* 2022. Vol. 60. N 7, p. 626-640. DOI: 10.31857/S0016702922070047

22. Kozlov N.E., Ivanov A.A., Nerovich L.I. The Lapland Granulite Belt: the primary nature and evolution. Apatity: KNTs AN SSSR, 1990, p. 168 (in Russian).

23. Vinogradov L.A., Bogdanova M.N., Efimov M.M. The Granulite Belt of the Kola Peninsula. Leningrad: Nauka, 1980, p. 208 (in Russian).

24. Safronov V.T., Rosen O.M. Metacarbonate Rocks (Calciphyres) of the Lapland-Kolvitsa Granulite Belt, Baltic Shield. *Lithology and Mineral Resources.* 2004. Vol. 39. N 5, p. 425-436.

25. Ivliev A.I. Geology of the Lapland granulite belt metamorphic terraines (Sal'nye Tundras, the Kola Peninsula): Avtoref. dis. … kand. geol.-mineral. nauk. Moscow: IMGRE, 1977, p. 23 (in Russian).

26. McCrea J.M. On the Isotopic Chemistry of Carbonates and a Paleotemperature Scale. *The Journal of Chemical Physics*. 1950. Vol. 18. N 6, p. 849-857. DOI: 10.1063/1.1747785

27. Clayton R.N., Mayeda T.K. The use of bromine pentafluoride in the extraction of oxygen from oxides and silicates for isotopic analysis. *Geochimica et Cosmochimica Acta.* 1963. Vol. 27. Iss. 1, p. 43-52. DOI: 10.1016/0016-7037(63)90071-1

28. Sang-Tae Kim, O'Neil J.R. Equilibrium and nonequilihrium oxygen isotope effects in synthetic carbonates. *Geochimica et Cosmochimica Acta*. 1997. Vol. 61. N 16, p. 3461-3475. DOI: 10.1016/s0016-7037(97)00169-5

29. Krylov D.P. Stable isotope fractionations involving Ca-Mg carbonates: evaluation of the β-factors by the "frozen phonon" method. *Geokhimiya*. 2022. Vol. 67. N 10, p. 942-960 (in Russian). DOI: 10.31857/S0016752522100065

30. Connoly J.A.D. Multivariable phase-diagrams – an algorithm based on generalized thermodynamics. *American Journal of Science*. 1990. Vol. 290. Iss. 6, p. 666-718. DOI: 10.2475/ajs.290.6.666

31. Connolly J.A.D. A Primer in Gibbs Energy Minimization for Geophysicists. *Petrology*. 2017. Vol. 25. N 5, p. 526-534. DOI: 10.1134/S0869591117050034

32. Hua Xiang, Connolly J.A.D. GeoPS: An interactive visual computing tool for thermodynamic modelling of phase equilibria. *Journal of Metamorphic Geology*. 2022. Vol. 40. Iss. 2, p. 243-255. DOI: 10.1111/jmg.12626

33. Holland T.J.B., Powell R. An internally consistent thermodynamic data set for phases of petrological interest. *Journal of Metamorphic Geology*. 1998. Vol. 16. N 3, p. 309-343. DOI: 10.1111/j.1525-1314.1998.00140.x

34. Bibikova E.V., Melnikov V.F., Avakyan K.Kh. The Lapland granulites: petrology, geochemistry, isotopic age. *Petrologiya*. 1993. Vol. 1. N 2, p. 215-234 (in Russian).

35. Mints M.V., Glaznev V.N., Konilov A.N. et al. The Lapland-Kolvitsa Granulite-Gneiss Belt. The Early Precambrian of the northeastern Baltic Shield: paleogeodynamics, crustal structure and evolution. Moscow: Nauchnyi Mir, 1996, p. 112-138 (in Russian).

36. Schidlowski M., Eichmann R., Junge C.E. Precambrian sedimentary carbonates: carbon and oxygen isotope geochemistry and implications for the terrestrial oxygen budget. *Precambrian Research.* 1975. Vol. 2. Iss. 1, p. 1-69. DOI: 10.1016/0301-9268(75)90018-2

37. Shields G., Veizer J. Precambrian marine carbonate isotope database: Version 1.1. *Geochemistry, Geophysics, Geosystems*. 2002. Vol. 3. N 6, p. 1-12. DOI: 10.1029/2001GC000266

38. Baumgartner L.P., Valley J.W. Stable Isotope Transport and Contact Metamorphic Fluid Flow. *Reviews in Mineralogy and Geochemistry*. 2001. Vol. 43. N 1, p. 415-467. DOI: 10.2138/gsrmg.43.1.415

39. Valley J.W. Stable isotope geochemistry of metamorphic rocks. Stable Isotopes in High Temperature Geological Processes. 1986, p. 445-490. DOI: 10.1515/9781501508936-018

40. Lattanzi P., Rye D.M., Rice J.M. Behavior of $^{13}C$ and $^{18}O$ in carbonates during contact metamorphism at Marysville, Montana: implications for isotope systematics in impure dolomitic limestones. *American Journal of Science*. 1980. Vol. 280, p. 890-906. DOI: 10.2475/ajs.280.9.890

41. Graf D.L. Geochemistry of Carbonate Sediments and Sedimentary Carbonate Rocks: Part IA-A. Isotopic Composition Chemical Analysis. Urbana: Illinois State Geological Survey, 1960, p. 42.

42. Hoefs J. Stable Isotope Geochemistry. Springer, 2015, p. 389. DOI: 10.1007/978-3-319-19716-6

***Authors*: Dmitrii P. Krylov**, *Doctor of Geological and Mineralogical Sciences, Leading Researcher, d.p.krylov@ipgg.ru, https://orcid.org/0000-0001-6654-8659* (*Institute of Precambrian Geology and Geochronology RAS, Saint Petersburg, Russia*), **Ekaterina V. Klimova,** *Junior Researcher, https://orcid.org/0000-0002-9771-9518* (*Institute of Precambrian Geology and Geochronology RAS, Saint Petersburg, Russia*).

*The authors declare no conflict of interests.*